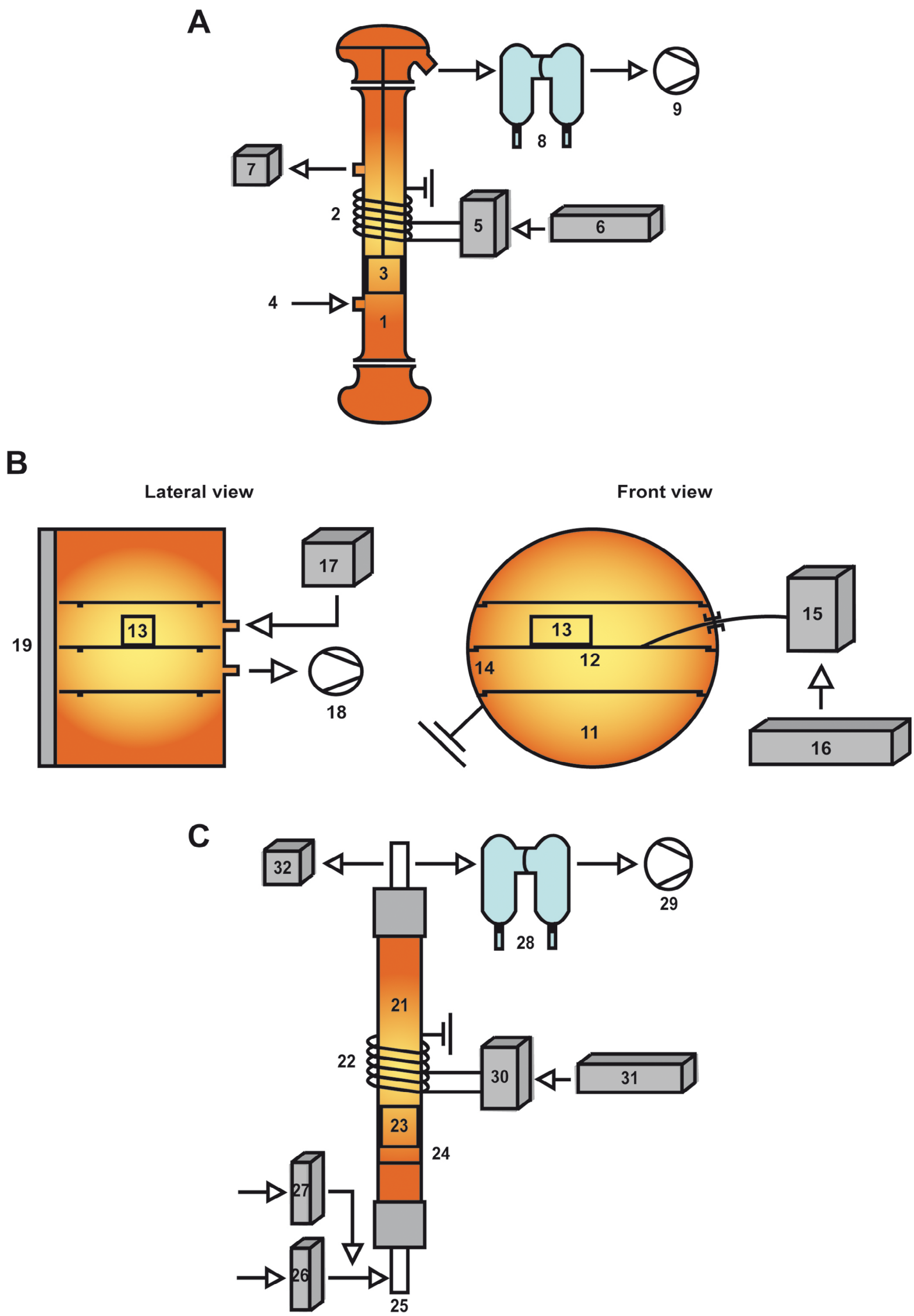
A
1
2
3
4
5
6
7
8
9
B
Lateral view
Front view
11
12
13
14
15
16
17
18
19
C
21
22
23
24
25
26
27
28
29
30
31
32

Figure 29: Shematics of the 3 plasma reactors used in this work.
(**A**) The central 10 cm wide glass tube (1) is where the plasma is generated by means of a copper coil (2), which is coupled to a Radio Frequency (RF = 13.56 MHz) pulsed generator (6). The generator is inductively coupled through the match box (5) to the coil, which is composed of eight turns of an 8 mm copper tube. The reactor tube has two small side openings, one for the entrance of the reactant gases (4) and one to measure the pressure inside the reactor using a pirani gauge (7). HA powders were placed on a vase (3) that was suspended to be near the copper coil, where plasma is generated. The upper round flask is connected to the vacuum system that includes a double cold trap (8) and the vacuum pump (9). (**B**) The glow discharge reactor consisted of a stainless steel discharge vessel (diameter: 26cm, length: 24cm) parallel plate reactor (11) with a stainless steel door (19). The ground electrode (14) was the reactor chamber, and the Radio Frequency (RF) electrode was a stainless steel plate (12). The samples (13) were located on this plate for plasma treatment. The RF electrode was connected to a RF pulse generator (16) through a matching network (15). The gases were supplied via a standard manifold (17) with gas fluxes adjusted with needle valves. The system pressure was determined using a Pirani type vacuum meter (MKS, USA), positioned between the reactor and the two stage mechanical vacuum pump (18). (**C**) The central part is a 30 mm wide glass tube (21). The microparticles (23) are supported on a porous plate (24) with a porosity that has strong influence on the fluidization conditions in the reactor. The copper coil (22) has 9 turns and is 2 mm wide. The tube is connected at the upper part to the pressure gauge (32) on one side and the cold trap (28) and the vacuum pump (29) on the other. A special design of the cold trap (28) allows prevention of the entrance of the powder in case this escapes from the reactor. The RF pulse generator (31) and the matching system (32) are the same as those explained above. A flow of argon (26) is mixed with the monomer coming from an evaporation unit (27) and used to fluidize the microparticles (23).

5.4.1.4. *Dispersibility assay to evaluate efficiency of the coatings of HA microparticles*

There were three types of particles to be evaluated; HA microparticles, HA microparticles coated with acrylic acid by plasma polymerization and, finally, HA microparticles coated with AMMO and acrylic acid. These coated microparticles were submitted to a deposition assay in order to determine the grade of attachment of the polymer coating. The deposition assay consists on suspending 12 mg of HA powder into Simulated Body Fluid (SBF), prepared as already described [28], and then plotting the light absorption versus time (λ = 450 nm). The decrease in light absorption is proportional to the ratio of particles suspended in the fluid and allows comparing the dispersibility of the studied microparticles. The absorption values are presented as a normalized value referred to the first value of absorption of each sample.

5.4.1.5. *Design of a Cold Plasma Fluidized Bed Reactor*

A new plasma fluidized bed reactor was designed in order to render homogenously coated microparticles. This reactor (see **Figure 29 C**) has a glass body tube (∅ = 30 mm) that is connected to an argon flow and a preheated monomer at the bottom and to a pressure gauge and a vacuum pump at the top. The vacuum line is provided with a cold trap that prevents the organic monomer as well as the particles from reaching the vacuum pump. In this reactor, cold plasma is generated by a radiofrequency altered inductive magnetic field. This altered magnetic field is obtained by surrounding the reactor with a nine-turn copper coil with 2 mm of diameter and connected to a power supply, which is in turn linked to a radiofrequency generator.

5.4.2. Surface coating of 96 well plates with Pentafluorophenyl Methacrylate (PFM)

5.4.2.1. Doehlert design to determine the best working conditions to perform grafting polymerization

The plasma grafting has two steps: first, the plate's surface is activated by an oxidizing plasma and then a solution of the monomer Pentafluorophenyl Methacrylate (PFM) diluted in acetonitrile is added to the wells to complete the reaction. Our group has intensive knowledge on the activation of organic surfaces with oxidizing plasma in a discharge plasma reactor (Francesch et al) so we focused on finding the best conditions in which the reaction between the activated surface and the PFM takes place.

The conditions for the reaction between PFM and the 96-well plate were optimized by response surface methodology (RSM) using a Doehlert design with two variables that were reaction time and PFM concentration. The Doehlert design is a multivariate second order design that is frequently used in experimental set-ups [139-143]. In our case, we decided to include five levels for reaction time between the solution of PFM and the plasma activated 96-well plate (15, 30, 45, 60, 75 minutes) and three levels for the concentration of PFM (55.7, 200 and 344.3 mM). In the Doehlert design the number of experiments is equal to $k^2+k+1+n$ being k the number of factors studied, 2 in our case, and n the number of repetitions planned in the design. We decided to perform one repetition for each point in the Doehlert matrix so in our design, $n = k^2+k+1$. Thus, the total number of experiments performed is 14.

With this setting, the Doehlert matrix of experiments is detailed in **Figure 30**. Each of these experimental points was repeated twice giving rise to the 14 experiments noted above.

[PFM] / mM	200	200	344.3	344.3	200	55.7	55.7
T reaction / min	45	75	60	30	15	30	60

Figure 30: Doehlert matrix of experiments.
This table represents the 7 points defining the experimental hexagon used in the Doehlert design. [PFM] is studied at 3 levels being 0 nM and 400 nM the experimental range. Time of reaction is studied at 5 levels between 15 and 75 minutes.

5.4.2.2. *Plasma activation of 96-well polystyrene plates*

The plasma apparatus consisted of a stainless steel discharge vessel (diameter: 26cm, length: 24cm) parallel plate reactor. The ground electrode was the reactor chamber, and the Radio Frequency (RF) electrode was a stainless steel plate placed in the middle of the reactor (**Figure 29 B**). Plasma was generated around the plate that served also as RF electrode and thus, the samples laid always on this plate for plasma-induced surface activation. The RF electrode was connected to a RF pulse generator (13.56 MHz) through a matching network.

The reactant gases (oxygen and argon mixture 99.999% pure) were introduced in the reaction chamber via standard manifolds and their pressure was adjusted with needle valves. The system pressure was determined using a Pirani pressure gauge (MKS, USA) located between the reactor and a cold trap that prevented monomers to enter the vacuum pump. A two-stages mechanical pump (RV12 903, Edwards, GB) generated the vacuum conditions needed to produce cold plasma. Operation conditions included a power setting of 100W with continuous radiofrequency supply, a final pressure of argon and oxygen of 0.1 - 0.4 mbar and 60 min of reaction time.

5.4.2.3. *Reaction between the plasma-activated plate and a solution of PFM*

The surface activated 96-well plate was placed in an argon hood to perform the reaction in inert atmosphere. Each well was filled with a solution of PFM (PC4318, Apollo Scientific) in acetonitrile (anhydrous, > 99,5% Sigma Aldrich 60004). Different concentrations were used in the reaction (55.7, 200 and 344.3 mM) following the Doehlert matrix design. The reaction time was also variable in the different wells also according to the Doehlert design: 15, 30, 45, 60 and 75 minutes. Removing the reaction cocktail stopped the reaction.

PFM fixation’s degree over the plate surface was determined by the reaction between PFM and glycine. So, after the PFM was fixed on the plate surface, the wells of the plate were washed with acetonitrile and soaked with a saturated glycine solution in acetonitrile. The attachment of glycine to the surface of the wells was analyzed by hydrolysis of the glycine in hydrochloric acid and further analysis by HPLC of the remnants of this hydrolytic cocktail.

5.4.2.4. *HPLC determination of glycine fixation over PFM modified plates*

The quantification of glycine by HPLC was performed with a C-18 reverse phase stationary column (Kromasil C18, Waters 2690) using a gradient mobile phase made of mixtures of three solvents: acetonitrile, water and a phosphate-acetate buffer. This buffer contained 0.14 M sodium acetate (S7670, Sigma), 17 mM triethylamine (T0886, Sigma) and phosphoric acid (85 %, 345245, Aldrich) and the working pH was 5.05 ± 0.02. The gradient used during the chromatograms was the following:

t (min)	Buffer (% $_{v/v}$)	Acetonitrile (% $_{v/v}$)
0-15	99	1
15-19	95	5
19-25	85	15
25-30	0	100

Figure 31: Mobile phase gradient used in the HPLC separation protocol of Glycine and Alanine

Alanine was added to all analyzed hydrolysis cocktails and used as internal standard for quantification. The alanine and glycine of the samples were both labeled with a fluorophore using accQ-Fluor Reagent Kit (WAT052880, Waters), following the manufacturer's instructions, to make the aminoacids visible to the fluorescent-based detector of the chromatographic system, (Alliance HPLC Waters 2695 module with a multi-λ fluorescent detector).

6. Conclusions

1. MEFs are multipotential cells capable of differentiating into other tissues of mesenchymal origin such as bone, cartilage and fat. Nevertheless, as cells need to be in a particular 3D environment in order to acquire all these phenotypes it can be concluded that the biological and biomechanical properties of the scaffold used for cell culture enhance fibroblast differentiation into other tissues.

2. MEFs cultured in the self-assembling peptide RAD16-I suffer a morphogenetic process similar to the mesenchymal condensation. Mechanical issues as well as expression of transcription factors support this conclusion. It has also been stated that the process is dependent on cell proliferation, tissue biomechanics and the presence of certain growth factors (PDGF and TGF-β). This model can be used as a preamble to a medicine based on regenerating systems similar to those of developmental processes.

3. MEFs cultured in RAD16-I have a default tendency to become chondrocyte-like cells, expressing genes like the sox trio or collagen type II. This intrinsic behavior of fibroblasts in RAD16-I opens the possibility of using this combination as a new strategy for cartilage repair. Moreover, this therapeutic approach has already proved safe once in animals because *In vivo* studies have shown that MEFs combined with RAD16-I have an excellent performance in mice in terms of cell viability and migration.

4. It is possible to produce a high diversity of hydroxyapatites combining the fact that Captal® is less dispersible than tailor-made HA and that an organic coating has different effects over Captal® or tailor-made HA. Moreover, a silane interface between HA and an acrylic coating doesn't affect the dispersibility of the particles so it can be inferred that the binding of HA and acrylic coatings is strong enough so that they are not significantly affected by a linking interface. Particular combinations of Captal®, tailor-made HA and coated samples of both will allow designing a stratified construct similar to the natural cartilage-to-bone interface in that calcium extracellular concentration and HA crystals will be different in different parts of the construct.

5. Finally, a novel process to produce plates suitable for combinatorial biological or biochemical assays has been developed. A Doehlert matrix design has optimized the experimental domain that most efficiently coats 96-well plates with PFM. This PFM enables to attach any biological molecule, which in turn allows to perform combinatorial experiments to find relevant peptides, sugars… for any particular application. Nevertheless, the use of an organic solvent partially degrades the polystyrene of the plate so water-based reactions or vapor grafting should be tried before scaling the process.

7. References

1. Wöhler F. Über Künstliche Bildung des Harnstoffs. Ann Phys Chem 1828;2(12):253-256.
2. Hoffman F, inventor; Bayer Co., assignee. Acetyl Salicylic Acid. US644077, 1900 02/27/1900.
3. Cohen SN, Chang AC, Boyer HW, Helling RB. Construction of biologically functional bacterial plasmids in vitro. Proc Natl Acad Sci U S A 1973 Nov;70(11):3240-3244.
4. Wu H. 3rd International Symposium on Antibody Engineering and Antibody-based Therapeutics (AEAT 2009). BiotechEast Co; 2009; Taipei; 2009.
5. Brookmeyer R, Johnson E, Ziegler-Graham K, Arrighi HM. Forecasting the global burden of Alzheimer's disease. Alzheimers & Dementia 2007;3:186-191.
6. Arthritis Foundation T. http://www.arthritis.org. 2009 [cited 2009 03/17/09]; Available from:
7. Stoick-Cooper CL, Moon RT, Weidinger G. Advances in signaling in vertebrate regeneration as a prelude to regenerative medicine. Genes Dev 2007 Jun 1;21(11):1292-1315.
8. Mikos AG, Herring SW, Ochareon P, Elisseeff J, Lu HH, Kandel R, et al. Engineering complex tissues. Tissue Eng 2006 Dec;12(12):3307-3339.
9. Sanchez C, Arribart H, Guille MM. Biomimetism and bioinspiration as tools for the design of innovative materials and systems. Nat Mater 2005 Apr;4(4):277-288.
10. Zhang S, Holmes TC, DiPersio CM, Hynes RO, Su X, Rich A. Self-complementary oligopeptide matrices support mammalian cell attachment. Biomaterials 1995 Dec;16(18):1385-1393.
11. Holmes TC, de Lacalle S, Su X, Liu G, Rich A, Zhang S. Extensive neurite outgrowth and active synapse formation on self-assembling peptide scaffolds. Proc Natl Acad Sci U S A 2000 Jun 6;97(12):6728-6733.
12. Semino CE, Kasahara J, Hayashi Y, Zhang S. Entrapment of migrating hippocampal neural cells in three-dimensional peptide nanofiber scaffold. Tissue Eng 2004 Mar-Apr;10(3-4):643-655.
13. Semino CE, Merok JR, Crane GG, Panagiotakos G, Zhang S. Functional differentiation of hepatocyte-like spheroid structures from putative liver progenitor cells in three-dimensional peptide scaffolds. Differentiation 2003 Jun;71(4-5):262-270.
14. Bobic V. New Methods for Repairing Articular Cartilage Damage In: Today M, editor. American Academy of Orthopaedic Surgeons Annual Meeting. Orlando, FL: Medscape Today, 2000.
15. Aastrom Biosciences I. Cell Therapies for Bone, Cardiac, Vascular and Neural Regeneration. 2009 [cited 2009 03/11/09]; Clinial Programs for bone regeneration using cell therapy]. Available from: http://www.aastrom.com/corporate/ClinicalPrograms.cfm

16. Dennis JE, Esterly K, Awadallah A, Parrish CR, Poynter GM, Goltry KL. Clinical-scale expansion of a mixed population of bone-marrow-derived stem and progenitor cells for potential use in bone-tissue regeneration. Stem Cells 2007 Oct;25(10):2575-2582.
17. Zurita M, Vaquero J, Bonilla C, Santos M, De Haro J, Oya S, et al. Functional recovery of chronic paraplegic pigs after autologous transplantation of bone marrow stromal cells. Transplantation 2008 Sep 27;86(6):845-853.
18. Cellerix. Ontaril: cell therapy based on Adipose Derived Stem Cells. 2009 [cited 2009 03/24/2009]; Available from: http://www.cellerix.com/Products/Ontaril
19. Fernández-Avilés. A Randomized Clinical Trial of Adipose-Derived Stem Cells in Treatment of Non Revascularizable Ischemic Myocardium. . PRECISE-01 Clinical Trial NCT00426868: Cytori Therapeutics; 2009.
20. Cytori Therapeutics. Cardiovascular Disease - Cell Therapy & Heart Disease. 2009 [cited 03/27/09]; Available from: http://www.cytoritx.com/intl/products/cv_stem_cells.html
21. Capone C, Frigerio S, Fumagalli S, Gelati M, Principato MC, Storini C, et al. Neurosphere-derived cells exert a neuroprotective action by changing the ischemic microenvironment. PLoS ONE 2007;2(4):e373.
22. Meissner KK, Kirkham DL, Doering LC. Transplants of neurosphere cell suspensions from aged mice are functional in the mouse model of Parkinson's. Brain Res 2005 Sep 28;1057(1-2):105-112.
23. Geron Inc. FDA clearance for Human Embryonic Stem Cell clinical trial for Spinal Cord repair. 2009 [cited 03/24/09]; Available from: http://www.geron.com/grnopc1clearance/
24. Brockes JP, Kumar A. Appendage regeneration in adult vertebrates and implications for regenerative medicine. Science 2005 Dec 23;310(5756):1919-1923.
25. Quintana L, Muinos TF, Genove E, Olmos MD, Borros S, Semino CE. Early Tissue Patterning Recreated by Mouse Embryonic Fibroblasts in a Three-Dimensional Environment. Tissue Eng Part A 2009;15(1):45-54.
26. Fernández T, Borrós S. Development of tailored hydroxyapatite. Master Thesis. Barcelona: Institut Químic de Sarrià, 2003.
27. Garreta E, Gasset D, Semino C, Borros S. Fabrication of a three-dimensional nanostructured biomaterial for tissue engineering of bone. Biomol Eng 2007 Feb;24(1):75-80.
28. Garreta E, Tricás N, Quintana L, Semino C, Borros S. Plasma Polymerization on Hydroxyapatite Powders to Increase Water Dispersability for Biomedical Applications. Plasma Processes and Polymers 2006;3(6-7):553-561.
29. Marí N, Borros S, Colominas C. Design and development of biomimetic surfaces. Master Thesis. Barcelona: Universitat Ramon Llull, 2007.
30. Hallmann A. Morphogenesis in the family Volvocaceae: different tactics for turning an embryo right-side out. Protist 2006 Oct;157(4):445-461.

31. Knecht DA, Fuller DL, Loomis WF. Surface glycoprotein, gp24, involved in early adhesion of Dictyostelium discoideum. Dev Biol 1987 May;121(1):277-283.
32. Michod RE. Evolution of individuality during the transition from unicellular to multicellular life. Proc Natl Acad Sci U S A 2007 May 15;104 Suppl 1:8613-8618.
33. Raper KB. Pseudoplasmodium formation and organization of *Dictyostelium discoideum.* J Elisha Mitchell Sci Soc 1940;56.
34. Endo T, Bryant SV, Gardiner DM. A stepwise model system for limb regeneration. Dev Biol 2004 Jun 1;270(1):135-145.
35. Gardiner DM, Bryant SV. The tetrapod Limb. In: Ferreti P, Geraudie J, editors. Cellular and Molecular Basis of Regeneration: from invertebrates to humans. Ltd. Chichester: John Wiley & Sons, 1998. p. 187-205.
36. Hopkinson-Woolley J, Hughes D, Gordon S, Martin P. Macrophage recruitment during limb development and wound healing in the embryonic and foetal mouse. J Cell Sci 1994 May;107 (Pt 5):1159-1167.
37. Mullen LM, Bryant SV, Torok MA, Blumberg B, Gardiner DM. Nerve dependency of regeneration: the role of Distal-less and FGF signaling in amphibian limb regeneration. Development 1996 Nov;122(11):3487-3497.
38. Zenjari C, Boilly B, Hondermarck H, Boilly-Marer Y. Nerve-blastema interactions induce fibroblast growth factor-1 release during limb regeneration in Pleurodeles waltl. Dev Growth Differ 1997 Feb;39(1):15-22.
39. Bokhari MA, Akay G, Zhang S, Birch MA. The enhancement of osteoblast growth and differentiation in vitro on a peptide hydrogel-polyHIPE polymer hybrid material. Biomaterials 2005 Sep;26(25):5198-5208.
40. Genove E, Shen C, Zhang S, Semino CE. The effect of functionalized self-assembling peptide scaffolds on human aortic endothelial cell function. Biomaterials 2005 Jun;26(16):3341-3351.
41. Kisiday J, Jin M, Kurz B, Hung H, Semino C, Zhang S, et al. Self-assembling peptide hydrogel fosters chondrocyte extracellular matrix production and cell division: implications for cartilage tissue repair. Proc Natl Acad Sci U S A 2002 Jul 23;99(15):9996-10001.
42. Narmoneva DA, Vukmirovic R, Davis ME, Kamm RD, Lee RT. Endothelial cells promote cardiac myocyte survival and spatial reorganization: implications for cardiac regeneration. Circulation 2004 Aug 24;110(8):962-968.
43. Werb Z. ECM and cell surface proteolysis: regulating cellular ecology. Cell 1997 Nov 14;91(4):439-442.
44. Zhang S, Rich A. Direct conversion of an oligopeptide from a beta-sheet to an alpha-helix: a model for amyloid formation. Proc Natl Acad Sci U S A 1997 Jan 7;94(1):23-28.

45. Garreta E, Genove E, Borros S, Semino CE. Osteogenic differentiation of mouse embryonic stem cells and mouse embryonic fibroblasts in a three-dimensional self-assembling peptide scaffold. Tissue Eng 2006 Aug;12(8):2215-2227.
46. Gourevitch D, Clark L, Chen P, Seitz A, Samulewicz SJ, Heber-Katz E. Matrix metalloproteinase activity correlates with blastema formation in the regenerating MRL mouse ear hole model. Dev Dyn 2003 Feb;226(2):377-387.
47. Ducy P, Zhang R, Geoffroy V, Ridall AL, Karsenty G. Osf2/Cbfa1: a transcriptional activator of osteoblast differentiation. Cell 1997 May 30;89(5):747-754.
48. Bielby RC, Boccaccini AR, Polak JM, Buttery LD. In vitro differentiation and in vivo mineralization of osteogenic cells derived from human embryonic stem cells. Tissue Eng 2004 Sep-Oct;10(9-10):1518-1525.
49. Buttery LD, Bourne S, Xynos JD, Wood H, Hughes FJ, Hughes SP, et al. Differentiation of osteoblasts and in vitro bone formation from murine embryonic stem cells. Tissue Eng 2001 Feb;7(1):89-99.
50. Cao T, Heng BC, Ye CP, Liu H, Toh WS, Robson P, et al. Osteogenic differentiation within intact human embryoid bodies result in a marked increase in osteocalcin secretion after 12 days of in vitro culture, and formation of morphologically distinct nodule-like structures. Tissue Cell 2005 Aug;37(4):325-334.
51. Jaiswal N, Haynesworth SE, Caplan AI, Bruder SP. Osteogenic differentiation of purified, culture-expanded human mesenchymal stem cells in vitro. J Cell Biochem 1997 Feb;64(2):295-312.
52. Lengner CJ, Lepper C, van Wijnen AJ, Stein JL, Stein GS, Lian JB. Primary mouse embryonic fibroblasts: a model of mesenchymal cartilage formation. J Cell Physiol 2004 Sep;200(3):327-333.
53. Pittenger MF, Mackay AM, Beck SC, Jaiswal RK, Douglas R, Mosca JD, et al. Multilineage potential of adult human mesenchymal stem cells. Science 1999 Apr 2;284(5411):143-147.
54. Stein GS, Lian JB. Molecular mechanisms mediating proliferation/differentiation interrelationships during progressive development of the osteoblast phenotype. Endocr Rev 1993 Aug;14(4):424-442.
55. Tai G, Polak JM, Bishop AE, Christodoulou I, Buttery LD. Differentiation of osteoblasts from murine embryonic stem cells by overexpression of the transcriptional factor osterix. Tissue Eng 2004 Sep-Oct;10(9-10):1456-1466.
56. Tchoukalova YD, Harteneck DA, Karwoski RA, Tarara J, Jensen MD. A quick, reliable, and automated method for fat cell sizing. J Lipid Res 2003 Sep;44(9):1795-1801.
57. Liu X, Wen FQ, Kobayashi T, Abe S, Fang Q, Piek E, et al. Smad3 mediates the TGF-beta-induced contraction of type I collagen gels by mouse embryo fibroblasts. Cell Motil Cytoskeleton 2003 Mar;54(3):248-253.

58. Tingstrom A, Heldin CH, Rubin K. Regulation of fibroblast-mediated collagen gel contraction by platelet-derived growth factor, interleukin-1 alpha and transforming growth factor-beta 1. J Cell Sci 1992 Jun;102 (Pt 2):315-322.
59. Ataliotis P. Platelet-derived growth factor A modulates limb chondrogenesis both in vivo and in vitro. Mech Dev 2000 Jun;94(1-2):13-24.
60. Quintana L, Zur Nieden NI, Semino CE. Morphogenetic and Regulatory Mechanisms during Developmental Chondrogenesis: New Paradigms for Cartilage Tissue Engineering. Tissue Eng Part B Rev 2008 Dec 8.
61. Zagai U, Fredriksson K, Rennard SI, Lundahl J, Skold CM. Platelets stimulate fibroblast-mediated contraction of collagen gels. Respir Res 2003;4:13.
62. Goldring MB, Tsuchimochi K, Ijiri K. The control of chondrogenesis. J Cell Biochem 2006 Jan 1;97(1):33-44.
63. Shen G, Darendeliler MA. The adaptive remodeling of condylar cartilage---a transition from chondrogenesis to osteogenesis. J Dent Res 2005 Aug;84(8):691-699.
64. Olsen BR, Reginato AM, Wang W. Bone development. Annu Rev Cell Dev Biol 2000;16:191-220.
65. Akiyama H, Chaboissier MC, Martin JF, Schedl A, de Crombrugghe B. The transcription factor Sox9 has essential roles in successive steps of the chondrocyte differentiation pathway and is required for expression of Sox5 and Sox6. Genes Dev 2002 Nov 1;16(21):2813-2828.
66. Kawakami Y, Rodriguez-Leon J, Belmonte JC. The role of TGFbetas and Sox9 during limb chondrogenesis. Curr Opin Cell Biol 2006 Dec;18(6):723-729.
67. Kou I, Ikegawa S. SOX9-dependent and -independent transcriptional regulation of human cartilage link protein. J Biol Chem 2004 Dec 3;279(49):50942-50948.
68. Sahar DE, Longaker MT, Quarto N. Sox9 neural crest determinant gene controls patterning and closure of the posterior frontal cranial suture. Dev Biol 2005 Apr 15;280(2):344-361.
69. Lefebvre V, Behringer RR, de Crombrugghe B. L-Sox5, Sox6 and Sox9 control essential steps of the chondrocyte differentiation pathway. Osteoarthritis Cartilage 2001;9 Suppl A:S69-75.
70. Poole AR, Kojima T, Yasuda T, Mwale F, Kobayashi M, Laverty S. Composition and structure of articular cartilage: a template for tissue repair. Clin Orthop Relat Res 2001 Oct(391 Suppl):S26-33.
71. French MM, Smith SE, Akanbi K, Sanford T, Hecht J, Farach-Carson MC, et al. Expression of the heparan sulfate proteoglycan, perlecan, during mouse embryogenesis and perlecan chondrogenic activity in vitro. J Cell Biol 1999 May 31;145(5):1103-1115.
72. Kispert A, Ortner H, Cooke J, Herrmann BG. The chick Brachyury gene: developmental expression pattern and response to axial induction by localized activin. Dev Biol 1995 Apr;168(2):406-415.

73. Stemple DL. Structure and function of the notochord: an essential organ for chordate development. Development 2005 Jun;132(11):2503-2512.
74. Technau U. Brachyury, the blastopore and the evolution of the mesoderm. Bioessays 2001 Sep;23(9):788-794.
75. Gardiner DM, Endo T, Bryant SV. The molecular basis of amphibian limb regeneration: integrating the old with the new. Semin Cell Dev Biol 2002 Oct;13(5):345-352.
76. Denker AE, Haas AR, Nicoll SB, Tuan RS. Chondrogenic differentiation of murine C3H10T1/2 multipotential mesenchymal cells: I. Stimulation by bone morphogenetic protein-2 in high-density micromass cultures. Differentiation 1999 Jan;64(2):67-76.
77. Gomes RR, Jr., Joshi SS, Farach-Carson MC, Carson DD. Ribozyme-mediated perlecan knockdown impairs chondrogenic differentiation of C3H10T1/2 fibroblasts. Differentiation 2006 Feb;74(1):53-63.
78. Lefebvre V, Li P, de Crombrugghe B. A new long form of Sox5 (L-Sox5), Sox6 and Sox9 are coexpressed in chondrogenesis and cooperatively activate the type II collagen gene. EMBO J 1998 Oct 1;17(19):5718-5733.
79. Smits P, Dy P, Mitra S, Lefebvre V. Sox5 and Sox6 are needed to develop and maintain source, columnar, and hypertrophic chondrocytes in the cartilage growth plate. J Cell Biol 2004 Mar 1;164(5):747-758.
80. Smits P, Li P, Mandel J, Zhang Z, Deng JM, Behringer RR, et al. The transcription factors L-Sox5 and Sox6 are essential for cartilage formation. Dev Cell 2001 Aug;1(2):277-290.
81. Ichinose S, Tagami M, Muneta T, Sekiya I. Morphological examination during in vitro cartilage formation by human mesenchymal stem cells. Cell Tissue Res 2005 Nov;322(2):217-226.
82. Han Y, Lefebvre V. L-Sox5 and Sox6 drive expression of the aggrecan gene in cartilage by securing binding of Sox9 to a far-upstream enhancer. Mol Cell Biol 2008 Aug;28(16):4999-5013.
83. Stirpe NS, Goetinck PF. Gene regulation during cartilage differentiation: temporal and spatial expression of link protein and cartilage matrix protein in the developing limb. Development 1989 Sep;107(1):23-33.
84. Mundlos S, Meyer R, Yamada Y, Zabel B. Distribution of cartilage proteoglycan (aggrecan) core protein and link protein gene expression during human skeletal development. Matrix 1991 Nov;11(5):339-346.
85. Lin Z, Fitzgerald JB, Xu J, Willers C, Wood D, Grodzinsky AJ, et al. Gene expression profiles of human chondrocytes during passaged monolayer cultivation. J Orthop Res 2008 Sep;26(9):1230-1237.
86. Benya PD, Padilla SR, Nimni ME. Independent regulation of collagen types by chondrocytes during the loss of differentiated function in culture. Cell 1978 Dec;15(4):1313-1321.

87. Domm C, Schunke M, Christesen K, Kurz B. Redifferentiation of dedifferentiated bovine articular chondrocytes in alginate culture under low oxygen tension. Osteoarthritis Cartilage 2002 Jan;10(1):13-22.
88. Schulze-Tanzil G, de Souza P, Villegas Castrejon H, John T, Merker HJ, Scheid A, et al. Redifferentiation of dedifferentiated human chondrocytes in high-density cultures. Cell Tissue Res 2002 Jun;308(3):371-379.
89. Homicz MR, Chia SH, Schumacher BL, Masuda K, Thonar EJ, Sah RL, et al. Human septal chondrocyte redifferentiation in alginate, polyglycolic acid scaffold, and monolayer culture. Laryngoscope 2003 Jan;113(1):25-32.
90. Kawanishi M, Oura A, Furukawa K, Fukubayashi T, Nakamura K, Tateishi T, et al. Redifferentiation of dedifferentiated bovine articular chondrocytes enhanced by cyclic hydrostatic pressure under a gas-controlled system. Tissue Eng 2007 May;13(5):957-964.
91. Geyer G, Linss W. Toluidine blue staining of cartilage proteoglycan subunits. Acta Histochem 1978;61(1):127-134.
92. zur Nieden NI, Kempka G, Rancourt DE, Ahr HJ. Induction of chondro-, osteo- and adipogenesis in embryonic stem cells by bone morphogenetic protein-2: effect of cofactors on differentiating lineages. BMC Dev Biol 2005;5:1.
93. Czipri M, Otto JM, Cs-Szabo G, Kamath RV, Vermes C, Firneisz G, et al. Genetic rescue of chondrodysplasia and the perinatal lethal effect of cartilage link protein deficiency. J Biol Chem 2003 Oct 3;278(40):39214-39223.
94. Hoffman AS. Classes of materials used in medicine. In: Ratner BD, Hoffman, A.S., Schoen, F.J., Lemons, J.E., editor. Biomaterials science. San Diego, CA: Elsevier Academic Press, 2004. p. pp. 67-233.
95. Cai Y, Liu, Y., Yan, W., Hu, Q., Tao, J., Zhang, M., Shi, Z. and Tang, R. Role of hydroxyapatite nanoparticle size in bone cell proliferation. Journal of Materials Chemistry 2007;17(36):3780.
96. LeGeros RZ. Biodegradation and bioresorption of calcium phosphate ceramics. Clin Mater 1993;14(1):65-88.
97. Oh S, Tobin E, Yang Y, Carnes DL, Jr., Ong JL. In vivo evaluation of hydroxyapatite coatings of different crystallinities. Int J Oral Maxillofac Implants 2005 Sep-Oct;20(5):726-731.
98. van Blitterswijk CA, Hesseling SC, Grote JJ, Koerten HK, de Groot K. The biocompatibility of hydroxyapatite ceramic: a study of retrieved human middle ear implants. J Biomed Mater Res 1990 Apr;24(4):433-453.
99. Xue W, Tao S, Liu X, Zheng X, Ding C. In vivo evaluation of plasma sprayed hydroxyapatite coatings having different crystallinity. Biomaterials 2004 Feb;25(3):415-421.
100. Burgeson RE, Nimni ME. Collagen types. Molecular structure and tissue distribution. Clin Orthop Relat Res 1992 Sep(282):250-272.

101. Peggion E, Cosani A, Terbojevich M, Borin G. Conformational studies on polypeptides. The effect of sodium perchlorate on the conformation of poly-L-lysine and of random copolymers of L-lysine and L-phenylalanine in aqueous solution. Biopolymers 1972 Mar;11(3):633-643.

102. Rippon WB, Chen HH, Walton AG. Spectroscopic characterization of poly(Glu-Ala). J Mol Biol 1973 Apr 5;75(2):369-375.

103. Seipke G, Arfmann HA, Wagner KG. Synthesis and properties of alternating poly(Lys-Phe) and comparison with the random copolymer poly(Lys 51, Phe 49). Biopolymers 1974;13(8):1621-1633.

104. Misawa H, Kobayashi N, Soto-Gutierrez A, Chen Y, Yoshida A, Rivas-Carrillo JD, et al. PuraMatrix facilitates bone regeneration in bone defects of calvaria in mice. Cell Transplant 2006;15(10):903-910.

105. Sodian R, Sperling JS, Martin DP, Egozy A, Stock U, Mayer JE, Jr., et al. Fabrication of a trileaflet heart valve scaffold from a polyhydroxyalkanoate biopolyester for use in tissue engineering. Tissue Eng 2000 Apr;6(2):183-188.

106. Webb AR, Yang J, Ameer GA. Biodegradable polyester elastomers in tissue engineering. Expert Opin Biol Ther 2004 Jun;4(6):801-812.

107. Derose CM, De, A., Loening, A.M., Ray, P., Chatziioannou, A.F. and Gambhir, S.S. Multimodality imaging of tumour xenografts and metastases in mice with combined small-animal PET, small-animal CT, and bioluminescence imaging. J Nucl Med 2007;28:2718-2728.

108. Saditok RT, Blackwell, T.S. Bioluminescence imaging. Proc Am Thorac Soc 2005;2:537-540.

109. Dégano IR, Vilalta M, Bago JR, Matthies AM, Hubbell JA, Dimitriou H, et al. Bioluminescence imaging of calvarial bone repair using bone marrow and adipose tissue-derived mesenchymal stem cells. Biomaterials 2008 Feb;29(4):427-437.

110. Román I, Vilalta M, Rodriguez J, Matthies AM, Srouji S, Livne E, et al. Analysis of progenitor cell-scaffold combinations by in vivo non-invasive photonic imaging. Biomaterials 2007 Jun;28(17):2718-2728.

111. Lee HS, Teng SW, Chen HC, Lo W, Sun Y, Lin TY, et al. Imaging human bone marrow stem cell morphogenesis in polyglycolic acid scaffold by multiphoton microscopy. Tissue Eng 2006 Oct;12(10):2835-2841.

112. Narmoneva DA, Oni O, Sieminski AL, Zhang S, Gertler JP, Kamm RD, et al. Self-assembling short oligopeptides and the promotion of angiogenesis. Biomaterials 2005 Aug;26(23):4837-4846.

113. Polak J, Hench L. Gene therapy progress and prospects: in tissue engineering. Gene Ther 2005 Dec;12(24):1725-1733.

114. Rickert D, Moses MA, Lendlein A, Kelch S, Franke RP. The importance of angiogenesis in the interaction between polymeric biomaterials and surrounding tissue. Clin Hemorheol Microcirc 2003;28(3):175-181.

115. Fellah BH, Josselin N, Chappard D, Weiss P, Layrolle P. Inflammatory reaction in rats muscle after implantation of biphasic calcium phosphate micro particles. J Mater Sci Mater Med 2007 Feb;18(2):287-294.

116. Yoon SJ, Kim SH, Ha HJ, Ko YK, So JW, Kim MS, et al. Reduction of inflammatory reaction of poly(d,l-lactic-co-glycolic Acid) using demineralized bone particles. Tissue Eng Part A 2008 Apr;14(4):539-547.

117. Rubio N, Villacampa MM, El Hilali N, Blanco J. Metastatic burden in nude mice organs measured using prostate tumor PC-3 cells expressing the luciferase gene as a quantifiable tumor cell marker. Prostate 2000 Jul 1;44(2):133-143.

118. Kim MS, Kim SK, Kim SH, Hyun H, Khang G, Lee HB. In vivo osteogenic differentiation of rat bone marrow stromal cells in thermosensitive MPEG-PCL diblock copolymer gels. Tissue Eng 2006 Oct;12(10):2863-2873.

119. Garvey W. Modified elastic tissue-Masson trichrome stain. Stain Technol 1984 Jul;59(4):213-216.

120. Thomas E, Lochte H, Lu W, Ferrebee J. Intravenous infusion of bone marrow in patients receiving radiation and chemotherapy. N Engl J Med 1957;257:491-496.

121. Giordano A, Galderisi U, Marino IR. From the laboratory bench to the patient's bedside: an update on clinical trials with mesenchymal stem cells. J Cell Physiol 2007 Apr;211(1):27-35.

122. Hohaus C, Ganey TM, Minkus Y, Meisel HJ. Cell transplantation in lumbar spine disc degeneration disease. Eur Spine J 2008 Dec;17 Suppl 4:492-503.

123. TiGenix. http://www.tigenix.com/home2.asp?map=ab. 2009 [cited 15/03/09]; Available from:

124. Genzyme. http://www.genzyme.com/business/biz_home.asp. 2009 [cited 15/03/09]; Available from:

125. Athanasiou KA, Niederauer GG, Agrawal CM. Sterilization, toxicity, biocompatibility and clinical applications of polylactic acid polyglycolic acid copolymers. Biomaterials 1996;17(2):93-102.

126. Temenoff JS, Mikos AG. Review: tissue engineering for regeneration of articular cartilage. Biomaterials 2000;21(5):431-440.

127. Yaszemski MJ, Payne RG, Hayes WC, Langer R, Mikos AG. Evolution of bone transplantation: Molecular, cellular and tissue strategies to engineer human bone. Biomaterials 1996;17(2):175-185.

128. Dupraz AMP, deWijn JR, vanderMeer SAT, deGroot K. Characterization of silane-treated hydroxyapatite powders for use as filler in biodegradable composites. Journal of Biomedical Materials Research 1996;30(2):231-238.

129. De Bartolo L, Morelli S, Lopez LC, Giorno L, Campana C, Salerno S, et al. Biotransformation and liver-specific functions of human hepatocytes in culture on RGD-immobilized plasma-processed membranes. Biomaterials 2005;26(21):4432-4441.

130. Feng XF, Zhang J, Xie HK, Hu QH, Huang Q, Liu WW. The RF plasma polymer of lysine and the growth of human nerve cells on its surface. Surface & Coatings Technology 2003;171(1-3):96-100.
131. France RM, Short RD, Duval E, Jones FR, Dawson RA, MacNeil S. Plasma copolymerization of allyl alcohol 1,7-octadiene: Surface characterization and attachment of human keratinocytes. Chemistry of Materials 1998;10(4):1176-1183.
132. Harsch A, Calderon J, Timmons RB, Gross GW. Pulsed plasma deposition of allylamine on polysiloxane: a stable surface for neuronal cell adhesion. Journal of Neuroscience Methods 2000;98(2):135-144.
133. Kelly JM, Daw R, Short RD, Brook IM. The effect of surface functional groups(oxygen/carbon) on the attachment of osteoblast-like cells to plasma polymers. Journal of Dental Research 1999;78(5):1064-1064.
134. Sardella E, Gristina R, Ceccone G, Gilliland D, Papadopoulou-Bouraoui A, Rossi F, et al. Control of cell adhesion and spreading by spatial microarranged PEO-like and pdAA domains. Surface & Coatings Technology 2005;200(1-4):51-57.
135. Eberhardt M, Mruk R, Zentel R, Theato P. Synthesis of pentafluorophenyl(meth)acrylate polymers: New precursor polymers for the synthesis of multifunctional materials. European Polymer Journal 2005;41(7):1569-1575.
136. Francesch L, Borros S, Knoll W, Forch R. Surface reactivity of pulsed-plasma polymerized pentafluorophenyl methacrylate (PFM) toward amines and proteins in solution. Langmuir 2007;23(7):3927-3931.
137. Francesch L, Garreta E, Balcells M, Edelman ER, Borros S. Fabrication of bioactive surfaces by plasma polymerization techniques using a novel acrylate-derived monomer. Plasma Processes and Polymers 2005;2(8):605-611.
138. Marí-Buyé N, O'Shaughnessy S, Colominas C, Semino C, Gleason K, Borrós S. Functionalized, Swellable Hydrogel Layers as a Platform for Cell Studies. Advanced Functional Materials 2009;19(1):NA.
139. Dutra RL, Maltez HF, Carasek E. Development of an on-line preconcentration system for zinc determination in biological samples. Talanta 2006 Apr 15;69(2):488-493.
140. Lemos VA, Baliza PX, Santos JS, Nunes LS, Jesus AA, Rocha ME. A new functionalized resin and its application in preconcentration system with multivariate optimization for nickel determination in food samples. Talanta 2005 Mar 31;66(1):174-180.
141. Mennini N, Furlanetto S, Maestrelli F, Pinzauti S, Mura P. Response surface methodology in the optimization of chitosan-Ca pectinate bead formulations. Eur J Pharm Sci 2008 Nov 15;35(4):318-325.
142. Robaina NF, Soriano S, Cassella RJ. Polyurethane foam loaded with SDS for the adsorption of cationic dyes from aqueous medium: Multivariate optimization of the loading process. J Hazard Mater 2009 Jan 19.

143. Korn MG, Dos Santos WP, Korn M, Ferreira SL. Optimisation of focused-microwave assisted digestion procedure for Kjeldahl nitrogen determination in bean samples by factorial design and Doehlert design. Talanta 2005 Feb 15;65(3):710-715.

144. Liu DM, Yang QZ, Troczynski T, Tseng WJJ. Structural evolution of sol-gel-derived hydroxyapatite. Biomaterials 2002;23(7):PII S0142-9612(0101)00295-00292.

145. Tricas N, Borros S. Carbon Black surface chemical modification by atmospheric plasma. Kgk-Kautschuk Gummi Kunststoffe 2005;58(10):511-517.

146. Hutmacher D, Schantz J, Lam C, Tan K, Lim T. State of the art and future directions of scaffold-based bone engineering from a biomaterials perspective. Journal of Tissue Engineering and Regenerative Medicine 2007;1(4):245-260.

147. Dorozhkina EI, Dorozhkin SV. Surface mineralisation of hydroxyapatite in modified simulated body fluid (mSBF) with higher amounts of hydrogencarbonate ions. Colloids and Surfaces A: Physicochemical and Engineering Aspects 2002;210(1):41-48.

148. Medina Ledo H, Thackray A, Jones I, Marquis P, Macaskie L, Sammons R. Microstructure and composition of biosynthetically synthesised hydroxyapatite. Journal of Materials Science: Materials in Medicine 2008;19(11):3419-3427.

149. Bikiaris D, Matzinos P, Larena A, Flaris V, Panayiotou C. Use of silane agents and poly(propylene-g-maleic anhydride) copolymer as adhesion promoters in glass fiber/polypropylene composites. Journal of Applied Polymer Science 2001;81(3):701-709.

150. Britcher L, Kempson S, Matisons J. Silanes on glass fibers - Adhesion promoters for composite applications. Adhesion Promotion Techniques: Technological Applications 1999;14:347-385.

151. Cave NG, Kinloch AJ. SELF-ASSEMBLING MONOLAYER SILANE FILMS AS ADHESION PROMOTERS. Polymer 1992;33(6):1162-1170.

152. Halliwell CM, Cass AEG. A factorial analysis of silanization conditions for the immobilization of oligonucleotides on glass surfaces. Analytical Chemistry 2001;73(11):2476-2483.

153. Tricas N, Vidal-Escales E, Borros S. The role of carbon black surface activity and specific surface area in the vulcanization reaction. Afinidad 2002;59(500):337-342.

8. Annexes